Amargosa Basin Ecological Conservation

Evaluating the Health of the Mesquite Bosque in the Amargosa Basin with Earth Observations

Spring 2025 | California – JPL
April 4th, 2025

Authors: Gabrielle Shen (Analytical Mechanics Associates), Alondra Gallegos (Analytical Mechanics Associates), Simon Ng (Analytical Mechanics Associates), Peter Blatchford (Analytical Mechanics Associates)

Abstract: Increased development and shifting water use patterns in the Amargosa Basin have disrupted the region's natural hydrology, threatening its riparian ecosystems and habitat of western honey mesquite (*Prosopis glandulosa* var. *torreyana*). The mesquite holds significant cultural value for the Timbisha Shoshone, who have traditionally harvested mesquite pods for sustenance. Recent poor harvests have raised concerns for the Tribe and for the U.S. Fish and Wildlife Service (USFWS), who aim to preserve the landscape's biodiversity. To address the restoration of the mesquite bosque, we partnered with the Timbisha Shoshone Tribe, the USFWS, and the Friends of the Amargosa Basin. The Friends of the Amargosa Basin's campaign for national monument status would facilitate the development of a comprehensive management plan, leading to more effective and localized conservation strategies. We utilized data from Landsat 4 Thematic Mapper (TM), Landsat 5 TM, Landsat 8 Operational Land Imager (OLI), Landsat 9 OLI-2, Sentinel-1 C band Synthetic Aperture Radar, Sentinel-2 Multi-Spectral Instrument, Soil Moisture Active Passive L-band radiometer, and Ecosystem Spaceborne Thermal Radiometer Experiment on Space Station to detect changes in vegetation health through evapotranspiration and the Normalized Difference Vegetation Index. While the groundwater dependence of this region—and specifically of the mesquite bosque—limited our analysis on hydrological change, we successfully used Earth observations to identify areas of increasing and decreasing mesquite health. These end products will assist partners in future conservation efforts of the mesquite bosque with the goal of leading to more effective and localized conservation strategies.

Key Terms: remote sensing, NDVI, Sentinel-2, mesquite bosque, Amargosa Basin, interferometry, evapotranspiration, hydrology

Advisors: Vicky Espinoza (NASA Jet Propulsion Laboratory, California Institute of Technology, UCLA Joint Institute for Regional Earth System Science and Engineering), Brandi Downs (NASA Jet Propulsion Laboratory, California Institute of Technology), Matthew Bonnema (NASA Jet Propulsion Laboratory, California Institute of Technology), Benjamin Holt (NASA Jet Propulsion Laboratory, California Institute of Technology)

Lead: Caroline Baumann (California – JPL)

1. Introduction

The Amargosa Basin lies between Death Valley and the Mojave Desert in California and Nevada (Figure 1). The basin's only free-flowing river is the Amargosa River, whose ephemeral and perennial flows support numerous endemic and endangered species (Pavelko & Damar, 2023), including the Amargosa vole (*Microtus californicus scirpensis*; Parker et al., 2018). Additionally, the river holds significant cultural and ecological value for the Timbisha Shoshone Tribe, whose ancestral lands rely on its springs and seeps for sustenance and biodiversity.

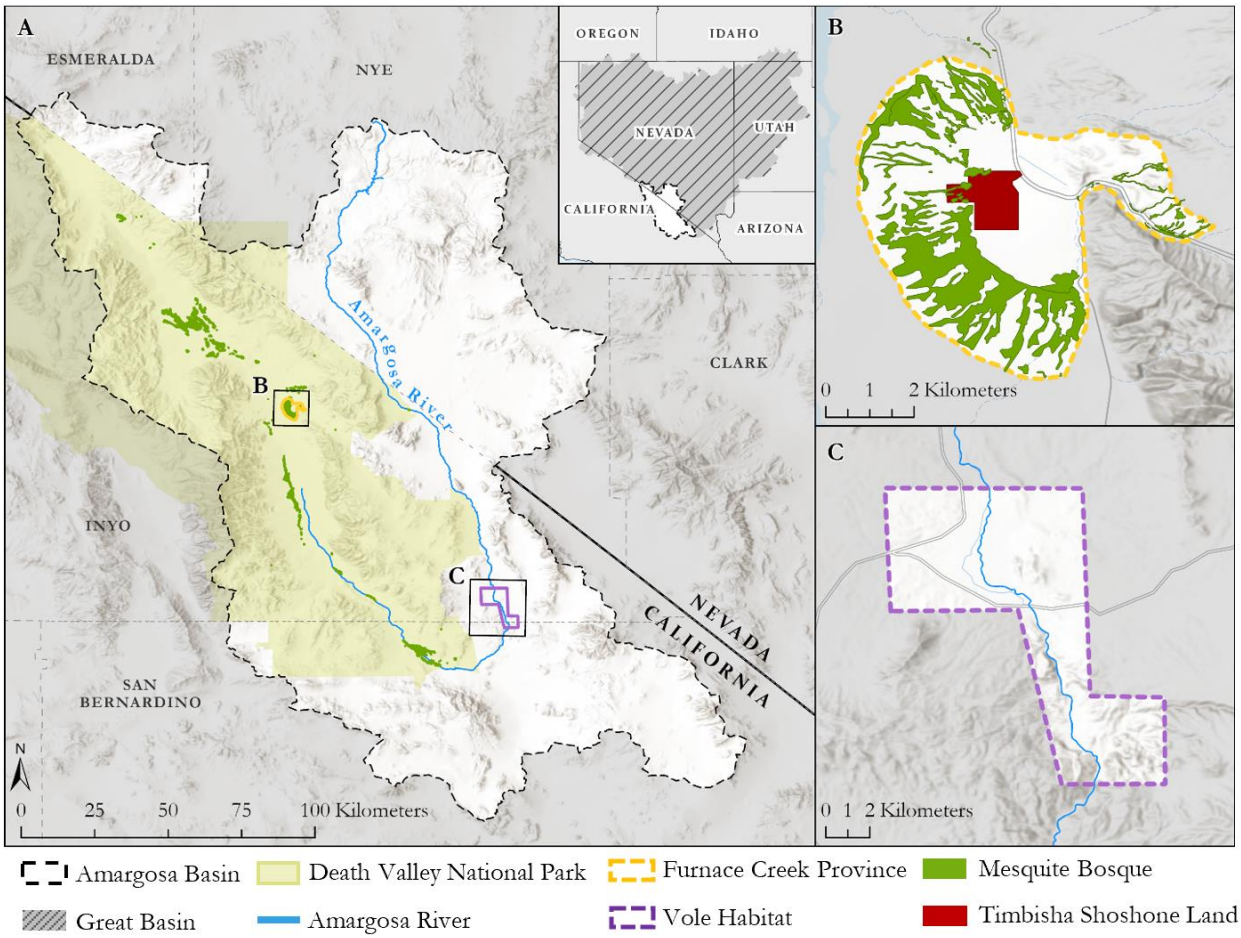

Figure 1. **A**) Regional view of the Amargosa Basin in Inyo and San Bernardino Counties, California, and Nye and Esmeralda Counties, Nevada. **B**) Furnace Creek Province. **C**) Vole Habitat.

Away from the Amargosa River riparian zones, isolated surface springs occupy an otherwise arid landscape. One of the few plant species able to survive this extreme environment is western honey mesquite (*Prosopis glandulosa* var. *Torreyana*), a phreatophyte with roots stretching to groundwater up to 18 meters below the surface (Orwa et al., 2009). Historically, the Timbisha Shoshone Tribe relied on the mesquite's nutritious pods for subsistence, and they continue to value it as part of their cultural identity (Fowler, 2019).
Over the last century, major anthropogenic hydrogeological alterations have threatened mesquite habitat. In 1927, developers constructed the Furnace Creek Inn (now The Oasis at Death Valley) and a golf course near one of the primary mesquite habitats and modern Timbisha Shoshone lands (*A Historical Chronology*, 2010). Later, engineers constructed a cement diversion dam to protect the property from floodwaters. More recently in 2017 and 2018, major renovations took place at The Oasis (*OZ Leads Major Renovations of the Historic "Oasis at Death Valley,"* 2018). The alteration of natural waterways and increased water demand by these developments have stressed soil moisture and groundwater availability in the area, likely contributing to a

decline in mesquite bosque health (Fowler, 2019; Campbell et al., 2017). Additionally, a warming climate has further increased evaporative demand, altered precipitation and recharge patterns, and prompted the systematic shift of water availability (Condon et al., 2020).

Among those concerned about the mesquite bosque are the Friends of the Amargosa Basin, the United States Fish & Wildlife Service (USFWS), and the Timbisha Shoshone Tribe, who all partnered with us on this project. The Friends of the Amargosa Basin is a 501(c)(3) nonprofit whose mission is to achieve national monument status for the Amargosa Basin. This would ensure a holistic management plan, protecting and honoring the land's broader historical, cultural, and ecological significance. The Timbisha Shoshone Tribe seeks to restore the mesquite bosque due to its historic cultural importance. The Tribe's focus on cultural restoration is complemented by the USFWS' priority of ecological conservation, which aims to promote biodiversity and protect endangered species. Currently, our partners participate in management efforts to protect the Amargosa region, restore its surrounding habitats, and increase public engagement. Additional collaborators included the National Park Service in Death Valley and the California Department of Fish and Wildlife.

Our team aimed to leverage remote sensing data in pursuit of four primary end products: a historic vegetation health change map, a more recent and higher resolution vegetation health change map, a soil moisture map, and a land subsidence map. Using these end products, our team's primary objective was to inform our partners' decision-making and conservation efforts, specifically related to water conservation and mesquite bosque restoration. Furthermore, we aimed to identify potential causes behind changes in vegetation health that we observed, such as increased development or changes in water availability. To investigate the effects of development and changes to mesquite bosque health, we set our study period from June 1984 through December 2024.

We evaluated mesquite health using spectral vegetation indices including Normalized Difference Vegetation Index (NDVI; Kriegler et al., 1969). Previous studies successfully distinguished mesquite from other species using Landsat 8 Operational Land Imager (OLI) at 30-meter (m) resolution and Sentinel-2 Multi-Spectral Instrument (MSI) at 10-m resolution coupled with a random forest machine learning model (Ng et al., 2016; Ng et al., 2017). We used Ecosystem Spaceborne Thermal Radiometer Experiment on Space Station (ECOSTRESS) data to evaluate evapotranspiration, another indicator of plant health. Water evaporation is an energy intensive process, so plant surface temperature measurably decreases as evapotranspiration rates increase. Thus, we utilized NASA ECOSTRESS' level 3 evapotranspiration and level 4 stress index product, based on the evaporative stress index (Otkin et al., 2013), to analyze mesquite plant health and response to water stress over time.

Past studies successfully used the L-band radiometer from the Soil Moisture Active Passive (SMAP) satellite to detect drought conditions and predict vegetation health (Mishra et al., 2017; Le et al., 2024). However, these studies often occurred on large spatial scales due to the 9-km resolution of SMAP data, while mesquite communities typically inhabit smaller areas. Combined with the 1-m depth limit on models from SMAP measurements, this limited the utility of SMAP in this study. Meanwhile, we evaluated changes in groundwater availability via land subsidence, measured by interferometric synthetic aperture radar (InSAR) (Liu et al., 2019). InSAR data was acquired from the C band Synthetic Aperture Radar (C-SAR) on Sentinel-1. Research on land subsidence in California's Central Valley had been expanded state-wide (unpublished work), and when coupled with knowledge about local hydrology and aquifer properties, inferences about groundwater change can be made.

2. Methodology

2.1 Data Acquisition

2.1.1 Vegetation Health

We utilized Landsat Collection 2, Tier 1 Level-2 Surface Reflectance data (Earth Resources Observation and Science [EROS] Center, 2020) from the United States Geological Survey (USGS) EarthExplorer (Table 1).

Specifically, we downloaded tiles at a 30-m resolution containing bands 3 and 4 from Landsat 4-5 and bands 4 and 5 from Landsat 8-9. These bands correspond to the red and near-infrared (NIR) surface reflectance bands of the satellites, respectively, and were taken from clear June and July days (< 10% cloud cover) for the entire study period. We left out data from 2012 due to the failure of a redundant gyroscope on Landsat 5 and the decommissioning of the satellite. Additional Landsat data was accessed from the SpatioTemporal Asset Catalog (STAC) hosted by Microsoft Planetary Computer. We wrote the script in Python v3.10.16 using the package pystac_client v0.8.5.

Table 1
Earth Observations

Imagery Source	Dataset	Parameters	Date Range	Source	Use
Landsat 4 Thematic Mapper (TM)	Collection 2 Level-2 Surface Reflectance	Surface Reflectance, NDVI	1989–1993	USGS EarthExplorer	Detect historical changes in NDVI at a 30-m resolution
Landsat 5 TM	Collection 2 Level-2 Surface Reflectance	Surface Reflectance, NDVI	1984–2011	USGS EarthExplorer	Detect historical changes in NDVI at a 30-m resolution
Landsat 8 OLI	Collection 2 Level-2 Surface Reflectance	Surface Reflectance, NDVI	2013–2024	USGS EarthExplorer	Detect historical changes in NDVI at a 30-m resolution
Landsat 9 OLI-2	Collection 2 Level-2 Surface Reflectance	Surface Reflectance, NDVI	2022–2024	USGS EarthExplorer	Detect historical changes in NDVI at a 30-m resolution
Sentinel-1 C-SAR	Interferometric Wide (IW) mode	Subsidence	2015–2019	Dr. Zhen Liu, JPL	Detect changes in surface elevation that can be interpreted to the fluctuation of groundwater tables
Sentinel-2 MSI	Level-2A Surface Reflectance	Surface Reflectance, NDVI	2017–2024	Earth Search by Element 84	Detect changes in land cover at a 10-m resolution
NAIP	Aerial imagery	Surface Reflectance, NDVI, Green Ratio	2005, 2009, 2010, 2012, 2014, 2016, 2018,	USGS EarthExplorer	Complement Sentinel-2 and Landsat NDVI values at a higher resolution

			2020, 2022		
ISS ECOSTRESS	ECO4ESIPTJPL Version 1	Evapotranspiration, Evaporative Stress Index	2019–2022	LP DAAC AppEEARS	Identify stressed vegetation
SMAP	L4_SM	Soil Moisture Anomaly	2015–2024	NASA Earthdata Search	Identify soil moisture in the upper 1-m of the soil column

Similarly, we used Sentinel-2's Multi-Spectral Instrument (MSI) at Level-2A from 2017 to 2024, with a resolution of 10-m. We accessed the data from the STAC maintained on Earth Search by Element 84 in the same way as Landsat. Images were selected over the month of July due to its dry conditions (*Weather - Death Valley National Park, U.S. National Park Service*, 2024), which should highlight mesquite in the landscape because other plants are less photosynthetically active at that time of year. We saved lists of valid images as GeoJSON files and used the links under 'assets' to access full-resolution images.

To complement our spectral Earth observation data for the Furnace Creek province, we acquired 1-m resolution aerial imagery from the National Agricultural Imagery Program (NAIP). These data are available on a semi-annual basis from 2010 to 2022, as well as in 2005 and in 2009. For each year that the U.S. Department of Agriculture's Farm Service Agency (FSA) collects these data, there are four tiles of imagery covering the Furnace Creek province, all acquired on the same date in either June or July.

In addition to our surface reflectance data, we assessed vegetation health and its response to water stress using ECOSTRESS Evapotranspiration (ET) PT-JPL Daily L3 Global 70-m (ECO3ETPTJPL) and Evaporative Stress Index (ESI) PT-JPL Daily L4 Global 70-m Version 1 (ECO4ESIPTJPL) products from 2019 to 2022. We acquired these images from NASA's Land Processes Distributed Active Archive Center's (LPDAAC) Application for Extracting and Exploring Analysis Ready Samples (AppEEARS). The ET and ESI data was generated using the Priestley-Taylor Jet Propulsion Laboratory (PT-JPL) algorithm, as detailed in their respective Algorithm Theoretical Basis Document (ATBD; Hook & Fisher, 2018 and 2019). ET is generated from the Level 2 data products for land surface temperature and emissivity, Level 1 geolocation information, and an array of ancillary data inputs. The PT-JPL algorithm derives ESI from the ratio of Level 3 actual evapotranspiration (ET) to potential evapotranspiration (PET). As an indicator of potential drought and plant water stress, ET and ESI have potential to highlight regions experiencing reduced plant productivity.

2.1.2 Hydrology

We acquired SMAP soil moisture data from NASA Earthdata Search to assess the role of upper soil water (i.e., upper 1-m of the soil column) availability on mesquite health. We utilized the Level 4 global 3-hourly root zone soil moisture at a 9-km resolution for our analysis. While the revisit time for SMAP is about four days, this product combines these orbital measurements with a land surface and precipitation model to update soil moisture estimates on three-hour cycles. Furthermore, while SMAP only directly senses measurements within the upper ~5-cm of the soil, these models allow soil moisture estimates to be expanded to the upper 1-m of the soil column. We downloaded this global dataset for every three hours of July from 2015–2024.

Pre-processed land subsidence data, a potential proxy for groundwater change, was graciously provided to us by Dr. Zhen Liu, a researcher at NASA's Jet Propulsion Laboratory (JPL). From Dr. Liu, we acquired a rate-of-change of land subsidence over the Amargosa Basin, calculated from Sentinel-1 C-SAR data from March 2015 to July 2019. This data was created according to the methods in Liu et al., 2019. To contextualize potential changes in water availability, we also acquired precipitation data for the years 2019–2022 from the National Weather Service's Western Region Headquarters' station in Furnace Creek.

2.2 Data Processing

2.2.1 Vegetation Health

For each year in our study period, we calculated median NDVI (Equation 1; Kriegler et al., 1969) using Python 3.12 and the red and NIR bands from Landsat 4, 5, 8, and 9. We also used ArcGIS Pro 3.3.0's Raster Calculator (Spatial Analyst) to find the overall median NDVI for the historical years of interest. Further processing in R 4.4.3 and RStudio was performed to visualize historical NDVI change throughout time.

$$\text{NDVI} = \frac{\text{NIR - Red}}{\text{NIR + Red}} \quad (1)$$

Additionally, we calculated NDVI according to Equation 1 from the red band-4 and NIR band-8 for each Sentinel-2 image. To mitigate the effect of day-to-day NDVI variation, occasional cloud cover, and other outlier values, we calculated the median NDVI value for each pixel from the images available for July of each year. Next, we mosaiced the three Sentinel-2 tiles covering the mesquite and vole habitats within the Amargosa Basin. Finally, we masked the mosaic composite NDVI image; our mask included the vole habitat near Tecopa, the Furnace Creek area, and a mesquite habitat shapefile shared by our USFWS partners with a 1-km buffer to generously include any mesquite growing near the provided shapefile.

We also used Equation 1 to calculate NDVI for our NAIP imagery. However, it was first necessary to mosaic together the four tiles covering the Furnace Creek area, align them between years, and resample rasters from years with an 0.6-m resolution (beginning in 2016) to match the 1-m resolution of earlier years. We excluded 2005 from our NDVI calculations using NAIP because no NIR band was available. We also calculated the Green Ratio for NAIP (G/R), including 2005 (Ng et al., 2017).

Similarly, we calculated the annual median composites for ET values and annual mean composites of ESI values using Python to create baselines for comparison. Because ESI is a calculated ratio value ranging from 0 to 1, a median composite was not the preferred method as it was for ET, since there are no extreme outliers to exclude. These composites allowed us to compare regions within the Amargosa Basin where vegetation may have experienced reduced or increased productivity over the course of the study period.

2.2.2 Hydrology

Our soil moisture data was heavily processed before download, with land surface models extrapolating soil moisture measurements to a one-meter depth and at a three-hourly temporal resolution. Therefore, no further processing steps were necessary. For land subsidence, Dr. Zhen Liu shared these data as a list of points with rate of subsidence in millimeters per year, spaced 0.01 degrees apart in latitude and longitude. We converted these points into a raster, with each pixel centering on each point's coordinates. This yielded a raster with pixels at approximately 1000-m resolution.

2.3 Data Analysis

2.3.1 Vegetation Health

To assess historical vegetation health change from our Landsat data, we identified the first and last year each pixel had an NDVI value above a threshold (NDVI > 0.1). We also hand-divided the Furnace Creek mesquite bosque into four regions: northeast, northwest, central, and southern. We divided the northeast and northwest regions along the airport runway and excluded the golf course and reservoir ponds from these regions. A sparsely vegetated strip separates the northwest and the central regions. We defined the southern region largely based on Timbisha Shoshone tribal members' comments that the southern section of the bosque grew relatively more recently than the rest of the bosque. Then, we summed the number of pixels with NDVI > 0.1 by region for each year and calculated the correlation coefficient, or R-value, between the years' pixel counts. R-values range from +1 to -1, where a larger positive or negative value indicates a stronger positive or negative correlation, respectively.

Additionally, we calculated a line-of-best-fit of the first order through the NDVI values of each pixel for the entire study period. The equation follows "y = mx+b" where "y" is the line-of-best-fit NDVI value, "m" is the NDVI rate-of-change, "x" is the year, and "b" is the intercept. We calculated rate-of-change using the "polyfit" function in numpy v2.1.3, and we added each pixel's slope (i.e. 'm') to a raster dataset. We also determined the anomaly from the overall median NDVI for each year to visualize change over time (Figure A1).

To evaluate vegetation health rate-of-change in more recent years, we created a raster of slopes for each pixel from 2017–2024 with our Sentinel-2 NDVI data in the same manner as the Landsat data. We also compared isolated mesquite stands throughout the Amargosa Basin, calculating statistics including mean NDVI to see how change in mesquite health varied spatially throughout the entire basin. We then performed these same rate-of-change calculations for our NAIP imagery from 2012–2022 to detect more subtle changes in mesquite extent that orbital sensors may miss. Using NAIP Green Ratio images, we also calculated the last year the Green Ratio was greater than 1.05 from 2005 to 2022. Additionally, to visualize how ET values have changed over the years, we subtracted the median composite images from their subsequent year (i.e. 2022 – 2021, etc.). These produced maps depicting the absolute difference in ET and identified areas that experienced either a net increase or decrease in productivity (Figure A7).

2.3.2 Hydrology

Using our processed SMAP data, we first created median soil moisture composites for July of each year from 2015–2024, as well as an overall median composite of this data. Then, we subtracted the yearly median composites from the overall median composite to produce yearly July soil moisture anomaly maps that indicate whether it was a relatively wet or dry July. To identify any temporal trends in the data, we used the same "polyfit" function in Python as with our Landsat and Sentinel-2 data to create a rate-of-change map for this period. We did not conduct any further analysis on the land subsidence data by itself, but we did utilize this data for inter-raster comparisons.

2.3.3 Inter-Raster Comparisons

In order to compare different parameters (dNDVI vs land subsidence, dNDVI vs soil moisture, and land subsidence vs soil moisture), we first resampled the higher-spatial-resolution raster to other raster's resolution by averaging using rioxarray v0.18.2 "reproject_match". Then, to conduct the comparison, we created scatter plots of each pixel's value for both rasters and calculated a line of best fit and coefficient of correlation.

3. Results

3.1 Analysis of Results

3.1.1 Vegetation Health

The northwest and northeast regions we delineated in the Furnace Creek mesquite bosque showed a large decline (Figure 2B), losing 1.8% and 2.4% of pixels with NDVI > 0.1 per year over the duration of the study period (1984 – 2024) with respect to the average pixel count from 1984 to 1988 (Table 2). Looking across the entire 40-year period, the northwest and northeast regions decline by 64% and 82% when comparing the average pixel count from the most recent 4 years (2020–2024) against that of the earliest 4 years (1984–1988). The central region does not decline in pixel count as consistently as the northern regions, which is reflected in the low R-value. Meanwhile, the southern region showed an increase in the pixel count for much of the 40-year span, which aligns with the experience of Timbisha Shoshone tribal members, who explained that the bosque's more southern region is relatively younger.

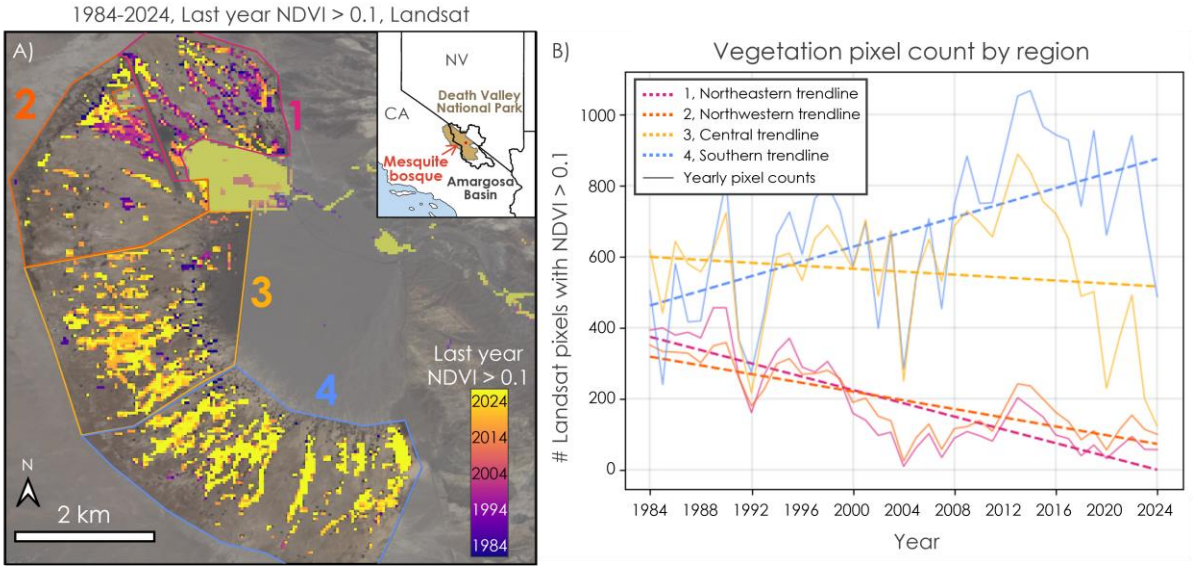

Figure 2. **A**) Map displaying the most recent year each Landsat pixel had an NDVI value greater than 0.1 in the Furnace Creek mesquite bosque. Superimposed are the 4 delineated regions for the vegetation pixel count. **B**) Graph showing the number of Landsat pixels with a NDVI value greater than 0.1 within each of the 4 regions. Solid lines are the yearly pixel counts, while the dotted lines are corresponding best-fit lines. The year 2012 was excluded from analysis because only Landsat 7 imagery with anomalous banding was available.

Table 2.
Change in vegetation pixel count in the Furnace Creek mesquite bosque

Region	1 Northeast	2 Northwest	3 Central	4 Southern	Total Study Area
Change in pixels / year	-9.3	-6.1	-2.1	+10.3	-7.2
R-value (-1 to +1)	-0.83	-0.78	-0.14	+0.58	-0.20
% Change / year with respect to the average 1984 to 1988	-2.4%	-1.8%	-0.4%	+2.4%	-0.4%
% Change from first 4 years to last 4 Years	-82%	-64%	-48%	+68%	-30%

Figure 2A provides additional spatiotemporal insight, showing the last year that each pixel had an NDVI value > 0.1 and revealing areas of potential new growth or mesquite death. Many pixels in the northern regions fell below an NDVI of 0.1 in the late 1990s and early 2000s, while there are more pixels in the central region that were last observed in the 2010s. Meanwhile, the southern region showed that more pixels were observed in 2024. Interestingly, there are pixels in the northern regions at the outer edge of the bosque that were present in 2024 and displayed increasing NDVI since 2017. We attempted to extend this analysis at higher spatial resolution using NAIP Green Ratio images. The last year with Green Ratio greater than 1.05 for each pixel shows similar trends as the Landsat analysis, though the NAIP data has greater year-to-year variability (Figure A10).

We also observed decreasing rate of change of NDVI in multiple regions of the Furnace Creek mesquite bosque from 1984 to 2024 (Figure 3), especially the areas north and northwest of the Xanterra golf course. Timbisha Shoshone Tribal Historic Preservation Officer Mandi Campbell explained that the mesquite near the golf course declined dramatically when the golf course's drainage reservoirs were moved to the northwest corner of the airport runway some decades ago. Southwest of the Timbisha Shoshone tribal land, there is another pocket of mesquite that exhibited overall declines in NDVI. However, there are some sections of mesquite that showed increasing NDVI, particularly in the southern extent of the mesquite bosque. The golf

course itself, as well as the nearby Furnace Creek Inn, demonstrated increasing NDVI over time, except for roadside areas of the golf course which experienced gradual development over this period (Figure A8). In addition, we evaluated the Furnace Creek mesquite bosque at greater spatial resolution using Sentinel-2 imagery, finding a decreasing NDVI in large swathes of the mesquite bosque from 2017 through 2024 (Figure 4). Declines in this analysis reflect dramatic declines in both the central and southern regions starting in 2013 (Figure 2B).

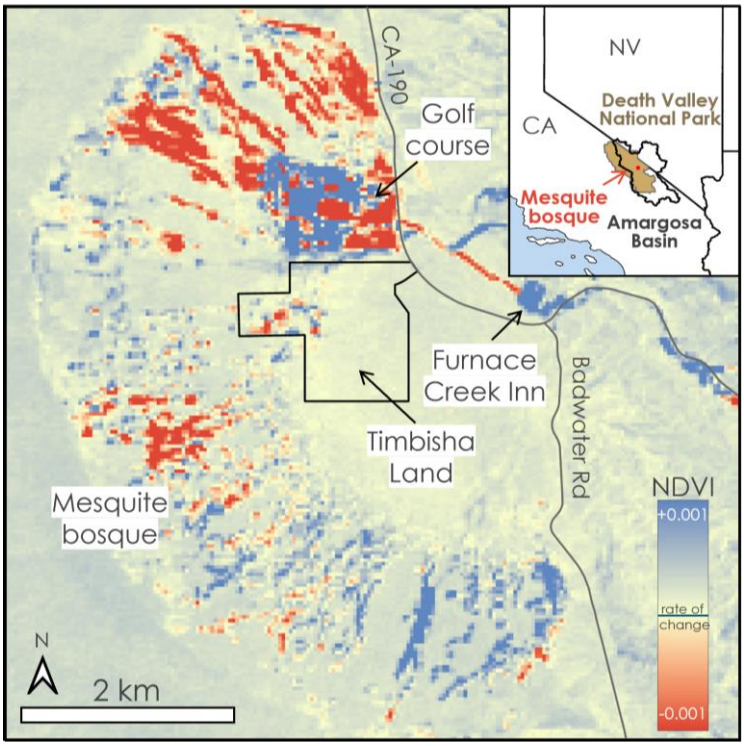

Figure 3. Furnace Creek mesquite bosque NDVI rate-of-change over 1984–2024 at 30-m resolution from Landsat 4, 5, 8, and 9.

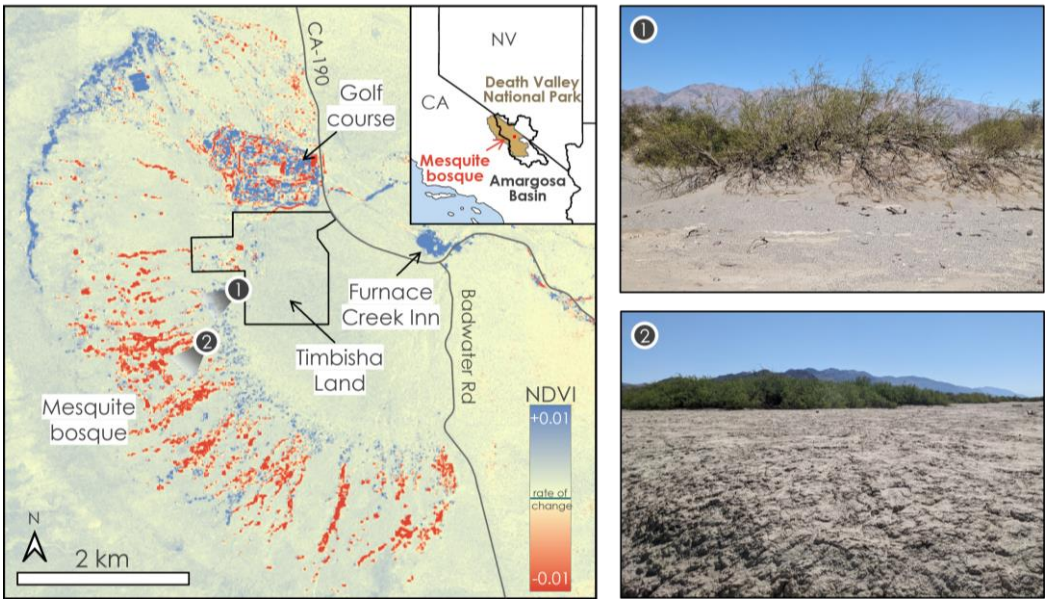

Figure 4. Map of Furnace Creek NDVI rate-of-change (2017-2024) at 10-m resolution from Sentinel-2. Images 1 and 2 were taken by Simon Ng on March 18th, 2025, with permission from the Timbisha Shoshone Tribe.

There were also isolated regions within the mesquite bosque that displayed increasing NDVI, primarily on the east edge of the bosque, as well as in the northwest. During our site visit on March 18th, 2025, we investigated the differences between the eastern edge of the bosque and the deeper bosque that is declining in health, pictured in Images 1 and 2 of Figure 4. Areas of increasing NDVI on the eastern edge of the bosque were sandy, with sand hummocks accumulating around the lower branches of mesquite trees. Further into the bosque where we saw decreasing NDVI, the soil was crustier and clay-like—each footstep would break through the crust into the fine powder underneath. National Park Service Botanist Rick McNeill explained that more saline soil can form the bumpier, puffy soil crust we observed in areas of decreasing NDVI. This analysis could be augmented with additional GIS data on soil composition.

We also compared the NDVI rate-of-change between Landsat and Sentinel-2, finding that they are highly correlated, with an R-value of 0.85 and the images look very similar (Figure A2). However, Sentinel-2 yielded NDVI rates-of-change ~1.5x higher than Landsat. Our NAIP-derived NDVI rate-of-change results generally support these trends in mesquite health (Figure A5), though we had less certainty in this dataset due to lower data availability.

We analyzed the ECOSTRESS data by comparing the median ET values across each year from 2019 to 2022 (Figure 5). In the Furnace Creek Province, ET remains consistently high within the golf course area likely due to frequent irrigation, whereas the surrounding mesquite bosque exhibits year-to-year variability. We believe that precipitation may be a primary driver for these observed trends, so we have produced a timeline of average monthly precipitation across this time frame (Figure B1, National Oceanic and Atmospheric Administration, 2025). The line graph in Figure B1 showed that rainfall was higher in 2021 and 2022 compared to 2019, therefore likely increasing surface water availability and temporarily boosting ET rates. The trends observed in ET are also true for ESI (Figure A9), indicating that where vegetation has higher ET values, they are less stressed and vice versa.

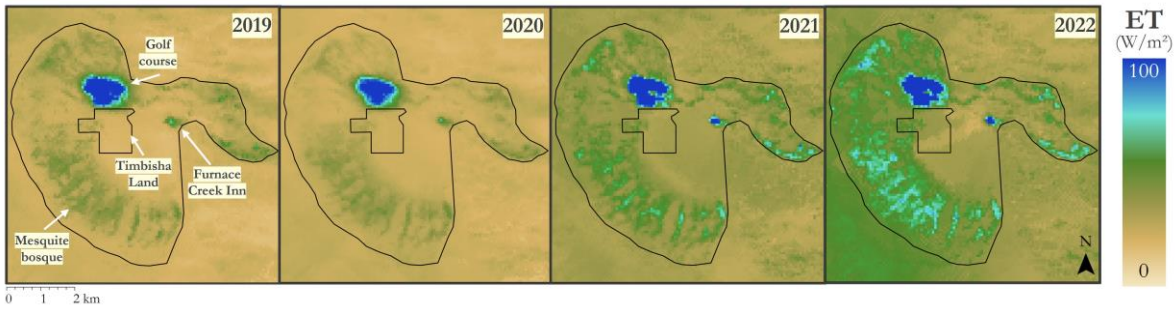

Figure 5. Furnace Creek mesquite bosque ET over 2019–2022 at 70-m resolution from ISS ECOSTRESS.

3.1.2 Hydrology

Our soil moisture data displayed high year-to-year variability in July soil moisture anomaly, with no clear trends in soil moisture over time (Figure 6). As a result, our rate-of-change analysis for soil moisture did not yield any statistically significant trends. While these longer-term trends may be present on larger timescales, over the ten-year time period of our SMAP data we interpreted changes in soil moisture to be driven by year-to-year precipitation variability. Furthermore, because our analysis only involved July data, not all precipitation events for each year (Figure B1) will be reflected in our results.

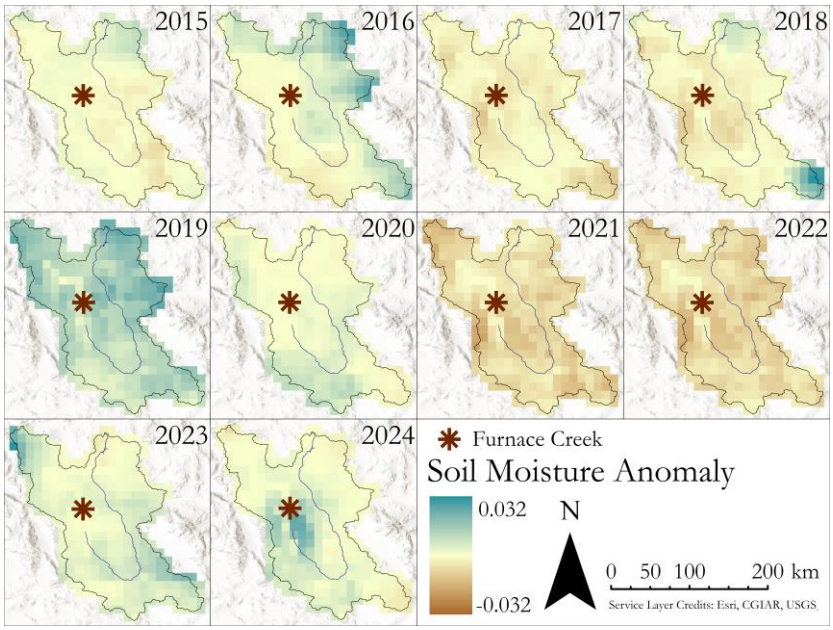

Figure 6. Soil Moisture Anomaly maps for July of each year from 2015–2024, with brown representing lower July soil moisture than the average year and blue higher.

Our land subsidence map showed one clear region with subsiding land around Furnace Creek (Figure 7). Elsewhere in the Amargosa Basin and Death Valley, there are zones of uplift and subsidence, but none as extensive as at Furnace Creek. When we visited Furnace Creek, National Park Service Botanist Rick McNeill explained that new groundwater wells were drilled at Travertine Springs on the east side of Furnace Creek. While land subsidence and groundwater depletion cannot be definitively linked from our data, the colocation of new wells and land subsidence is intriguing.

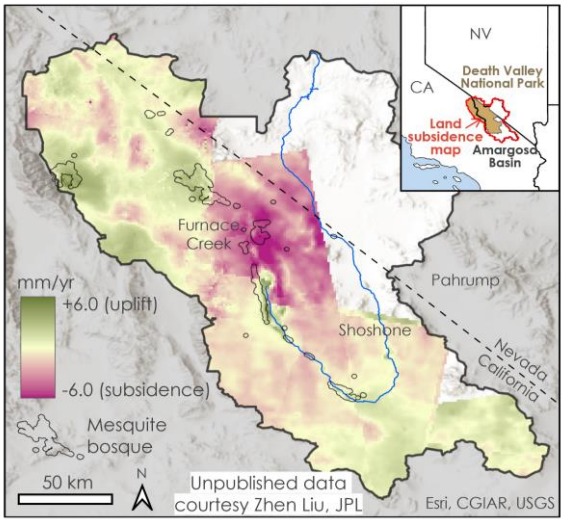

Figure 7. Average land subsidence over March 2015 to July 2019, calculated using Sentinel-1 C-SAR Interferometry data. Unpublished, pre-processed data provided courtesy Dr. Zhen Liu, JPL.

3.1.2 Raster Comparisons

Comparing the land subsidence data against the Sentinel-2 NDVI rate-of-change across the entire Amargosa Basin showed a weak-moderate correlation, with an R-value of 0.31 (Figure A3). Next, we compared the average soil moisture (2015–2024) to land subsidence or Sentinel-2 NDVI rate-of-change. We did not see any meaningful correlation between soil moisture and either land subsidence or NDVI rate-of-change, with R-values of -0.16 and -0.24, respectively (Figure A4).

3.2 Errors & Uncertainties

One major uncertainty that limited our analysis was the difficulty of detecting changes in water availability that would affect the mesquite bosque. Soil moisture is a commonly used parameter to assess water availability (Le et al., 2024), but because mesquite is a phreatophyte able to access deeper groundwater, soil moisture alone is not sufficient for this study. Furthermore, the 9-km spatial resolution of SMAP prevented us from analyzing soil moisture on a meaningful spatial scale. While the upcoming launch of NISAR would mark major improvements with resolutions up to 200-m (*Global NISAR soil moisture product*, 2024), there are no current remote sensing measurements of soil moisture on a comparable scale to Landsat or Sentinel imagery. Even with higher resolution measurements, there are also uncertainties surrounding the lag time between environmental factors like soil moisture and changes in vegetation health (Musyimi, 2011; Feng et al., 2023). Therefore, while we successfully detected yearly anomalies in July soil moisture (Figure 6), this was not able to effectively serve as a predictor of mesquite health.

Similar uncertainties about water availability were prevalent in our ET analysis, with the additional constraint of a limited spatiotemporal range of data. Because ECOSTRESS observations only cover part of 2018 through early 2023, we lack more recent data that could reveal continued declines in mesquite health. If groundwater pumping has intensified or if precipitation has decreased since 2022, current conditions may be considerably different from what is reflected in this analysis. Additionally, ET data coverage was inconsistent between images, with some images throughout the year missing large quantities of pixels or not covering sufficient area of our sites. Future data collection will be essential to determine whether the temporary improvements observed in 2021 and 2022 were short-lived and if mesquite stress has since worsened due to ongoing hydrological changes. This limitation underscores the importance of continued remote and in-situ monitoring to fully understand long-term trends in mesquite health.

To mitigate uncertainties surrounding our use of soil moisture and evapotranspiration, we utilized land subsidence as a means of detecting potential changes in groundwater availability (Liu et al., 2019). However,

this comes with its own uncertainties, as land subsidence and groundwater availability do not necessarily have a one-to-one correlation. Land subsidence can best act as a proxy for confined aquifers, but our limited knowledge of aquifer geometry and properties beneath the Amargosa Basin does not permit us complete certainty of our results. Furthermore, this data was only available to us as a rate-of-change between 2015–2019, ending before we would have expected to see a decrease in groundwater availability and potentially more local subsidence due to renovations at Furnace Creek.

In relation to our NDVI calculations, we also had uncertainty in detecting the isolated presence of mesquite. In the Furnace Creek province, we initially assumed that mesquite would be the dominant plant species within the alluvial fan in June and July. Our site visit and consultation with the Timbisha Shoshone Tribe, however, revealed that we might also be detecting the presence of "sneezeweed" (*Helenium autumnale*) or "arrowweed" (*Pluchea sericea*), two smaller brush-type plants that occur sporadically throughout the year. The resolution of Landsat and Sentinel data did not allow for object-based classification of what is and is not mesquite, so we acquired higher resolution NAIP imagery with this goal in mind.

However, there also existed potential uncertainty surrounding our use of NAIP imagery. First, the utility of this imagery for our purposes was limited by the low temporal availability of the data. Even when data were available, there were unexpected anomalies in our NDVI calculations that were not present in our Landsat and Sentinel data. In certain years, most noticeably in 2010 (Figure A6), there were regions with negative NDVI values over what appeared to be healthy mesquite from true color imagery. It is possible this is due to edge effects, or in years where this error is more prevalent, it may be due to shadows as the negative NDVI values were most observed on the western sides of mesquite trees. However, because NAIP images were available only every two years, we lacked imagery from nearby dates to assess whether our NDVI values were valid or reflected an underlying error.

4. Conclusions

4.1 Interpretation of Results

Our data revealed complexities in the potential drivers of mesquite health trends. While our NDVI results confirmed our partners' first-hand observations of declining mesquite health at Furnace Creek, these trends were spatially and temporally variable. For instance, the central mesquite pocket bordering the Timbisha Shoshone land displayed declining health—as indicated by lower NDVI—in both recent (~7 year) and historical (~40 year) analysis, while other areas of vegetation showed declines only in recent years or not at all. Overall, we found that mesquite health is a highly localized phenomenon, and our results will help our partners in taking informed conservation action on a local scale.

Identifying the drivers of mesquite health and explaining the observed declines in health posed its own challenges. Expanding our analysis beyond Furnace Creek to the entire Amargosa Basin, we identified weak to moderate correlations between land subsidence and NDVI. While this hints at a possible link between changing groundwater availability and mesquite health, a stronger understanding of aquifer geometry and increased in-situ data are necessary to be confident of groundwater's role here. Our evapotranspiration data also revealed contradicting trends in water stress, but there are complexities in using this metric for groundwater-dependent species that may have interfered with our analysis. The pattern we observed with high ET corresponding with higher-than-average precipitation suggests that mesquite may have relied more on shallow soil moisture from recent rainfall rather than deeper groundwater reserves. However, if groundwater depletion continues, soil moisture availability may decline, leading to lower ET and indicating increased plant stress. Therefore, to draw more concrete conclusions as to what has caused mesquite health decline, a comprehensive understanding of groundwater systems is essential.

4.2 Feasibility & Partner Implementation

This project provided insights into vegetation health, hydrological changes, and habitat conditions around the mesquite bosque, equipping our partners with data-driven products to enhance management and decision-making. Our Sentinel-2 mesquite health maps pinpointed areas of decline and potential recovery, allowing for

targeted conservation efforts. Additionally, our historical Landsat NDVI analyses offered long-term, regional context of vegetation health and can be used by partners to advocate for additional land and vegetation protections.

The evapotranspiration maps also identified areas of water stress that could impact sensitive species, providing reference to aid in future habitat management. Soil moisture findings revealed broader ecological variances, and despite complexities in aquifer geometry, land subsidence data revealed potential groundwater declines near Furnace Creek. Thus, our partners could utilize these products to emphasize the need for increased groundwater monitoring strategies.

Although direct remote sensing of groundwater-vegetation interactions remains complex, this project highlighted promising methods for integrating geospatial and in-situ aquifer data to support future conservation strategies. In the next project term, Earth observations will be used to detect seasonal differences in standing water and function as a metric to monitor viable habitat change for the highly endangered Amargosa vole.

5. Acknowledgements

We would like to acknowledge those who have contributed to the success of this project including,

NASA DEVELOP Program:

- Caroline Baumann (Center Lead, California – JPL)
- Laramie Plott (Senior Fellow, Virginia – Langley)

Science Advisors:

- Brandi Downs (NASA JPL, California Institute of Technology)
- Vicky Espinoza (NASA JPL, California Institute of Technology, UCLA Joint Institute for Regional Earth System Science and Engineering)
- Matthew Bonnema (NASA JPL, California Institute of Technology)
- Benjamin Holt (NASA JPL, California Institute of Technology)

Project Partners:

- Mandi Campbell (Tribal Historic Preservation Officer, Timbisha Shoshone Tribe)
- Cameron Mayer (Program Director, Friends of the Amargosa Basin)
- Christina Manville (U.S. Fish and Wildlife Service)
- Austin Roy (California Department of Fish and Wildlife)

Special Thanks:

- Rick McNeill (National Park Service, Death Valley NP)
- Susan Sorrells (President, Friends of the Amargosa Basin)

This material contains modified Copernicus Sentinel data (2015-2024), processed by ESA.

Any opinions, findings, and conclusions or recommendations expressed in this material are those of the author(s) and do not necessarily reflect the views of the National Aeronautics and Space Administration.

This material is based upon work supported by NASA through contract 80LARC23FA024.

6. Glossary

Bosque – Habitat found along the riparian flood plains of streams, riverbanks, and lakes

Earth observations – Satellites and sensors that collect information about the Earth's physical, chemical, and biological systems over space and time

ECOSTRESS – Ecosystem Spaceborne Thermal Radiometer Experiment on Space Station

Evaporative Stress Index (ESI) – Metric that describes temporal anomalies in evapotranspiration

Evapotranspiration (ET) – Process by which water is transferred from the land to the atmosphere by evaporation from soil and by transpiration from plants

Friends of the Amargosa Basin – Nonprofit organization dedicated to achieving monument status for the Amargosa Basin

Groundwater – Water present beneath Earth's surface in pores and crevices in rock

ISS – International Space Station

JPL – Jet Propulsion Laboratory

Land subsidence – Gradual settling or sudden sinking of the Earth's surface due to removal or displacement of subsurface Earth materials (e.g. groundwater)

Mesquite – Spiny tree or shrub of the pea family, native to arid regions of southwestern US and Mexico, that yields useful timber, tanbark, medicinal products, and edible pods

NAIP – National Agriculture Imagery Program

NISAR – NASA/Indian Space Research Organization Synthetic Aperture Radar

Normalized Difference Vegetation Index (NDVI) – Metric to quantify the health (greenness) and density of vegetation using sensor data

Phreatophyte – Plant with a deep root system that draws its water supply from the near water table

SMAP – Soil Moisture Active Passive

Timbisha Shoshone – Native American Tribe located in the Death Valley region, near the Nevada border

USFWS – United States Fish & Wildlife Service

7. References

A historical chronology (Backgrounder). (2010, October 4). The Oasis at Death Valley. https://www.oasisatdeathvalley.com/pressrelease/a-historical-chronology-backgrounder/

Campbell, J., Sharifi, M., & Rundel, P. (2017). Impact of Ground Water Depletion on the Mesquite Community at Edwards Air Force Base, Western Mojave Desert, California. *Aliso: A Journal of Systematic and Floristic Botany*, *35*(2), 69–77. https://doi.org/10.5642/aliso.20173502.03

Condon, L. E., Atchley, A.L. & Maxwell, R.M. (2020). Evapotranspiration depletes groundwater under warming over the contiguous United States. *Nature Communications*, *873*. https://doi.org/10.1038/s41467-020-14688-0

Earth Resources Observation and Science (EROS) Center. (2020). Landsat 4-5 Thematic Mapper Level-2, Collection 2 Surface Reflectance Bands 3-4. U.S. Geological Survey. https://doi.org/10.5066/P9IAXOVV.

Earth Resources Observation and Science (EROS) Center. (2020). Landsat 8-9 Operational Land Imager / Thermal Infrared Sensor Level-2, Collection 2 Surface Reflectance Bands 4-5. U.S. Geological Survey. https://doi.org/10.5066/P9OGBGM6.

European Space Agency. (2021). Copernicus Sentinel-2 MSI Collection 1 Level-2A Data [Data set]. https://doi.org/10.5270/S2_-znk9xsj

Feng, S., Zhang, Z., Zhao, S. et al. Time lag effect of vegetation response to seasonal precipitation in the Mara River Basin. Ecol Process 12, 49 (2023). https://doi.org/10.1186/s13717-023-00461-w

Fowler, C. S. (2019). Applied Ethnobiology and Advocacy: A Case Study from the Timbisha Shoshone Tribe of Death Valley, California. *Journal of Ethnobiology, 39*(1), 76-89. https://doi.org/10.2993/0278-0771-39.1.76.

Global NISAR soil moisture product. (2024, September 24). NASA Earthdata. https://www.earthdata.nasa.gov/about/nasa-support-snwg/solutions/global-nisar-soil-moisture

Hook, S., Fisher, J. (2019). ECOSTRESS Evaporative Stress Index PT-JPL Daily L4 Global 70 m V001 [Data set]. NASA EOSDIS Land Processes Distributed Active Archive Center. https://doi.org/10.5067/ECOSTRESS/ECO4ESIPTJPL.001

Hook, S., Fisher, J. (2018). ECOSTRESS Evapotranspiration PT-JPL Daily L3 Global 70 m V001 [Data set]. NASA EOSDIS Land Processes Distributed Active Archive Center. https://doi.org/10.5067/ECOSTRESS/ECO4ESIPTJPL.001

Kriegler, F., Malila, W., Nalepka, R., & Richardson, W. (1969). Preprocessing transformations and their effect on multispectral recognition. Proceedings of the 6th International Symposium on Remote Sensing of Environment. Ann Arbor, MI: University of Michigan, 97-131.

Le, M., Bolten, J. D., Whitney, K. M., Johnson, D. M., Mueller, R., & Mladenova, I. E. (2024). On the Use of SMAP Soil Moisture for Forecasting NDVI Over CONUS Cropland Regions. *Geophysical Research Letters*, *51*(20). https://doi.org/10.1029/2024gl111187

Liu, Z., Liu, P.-W., Massoud, E., Farr, T. G., Lundgren, P., & Famiglietti, J. S. (2019). Monitoring Groundwater Change in California's Central Valley Using Sentinel-1 and GRACE Observations. *Geosciences*, *9*(10), 436. https://doi.org/10.3390/geosciences9100436

Mishra, A., Vu, T., Veettil, A. V., & Entekhabi, D. (2017). Drought monitoring with soil moisture active passive (SMAP) measurements. *Journal of Hydrology, 552,* 620–632. https://doi.org/10.1016/j.jhydrol.2017.07.033

Musyimi, Z. (2011). Temporal relationships between remotely sensed soil moisture and NDVI over Africa : potential for drought early warning. https://essay.utwente.nl/84982/

National Oceanic and Atmospheric Administration, National Weather Service, Western Region Headquarters Observations at the Visitors Center at Furnace Creek Death Valley. (2025). https://www.weather.gov/wrh/timeseries?site=DEVC1&hours=72&units=english&chart=on&headers=on&obs=tabular&hourly=false&pview=standard&font=12&history=yes&start=20190101&end=20221231&plot=

Ng, W.-T., Meroni, M., Immitzer, M., Böck, S., Leonardi, U., Rembold, F., Gadain, H., & Atzberger, C. (2016). Mapping *Prosopis* spp. with Landsat 8 data in arid environments: Evaluating effectiveness of different methods and temporal imagery selection for Hargeisa, Somaliland. *International Journal of Applied Earth Observation and Geoinformation*, *53*, 76–89. https://doi.org/10.1016/j.jag.2016.07.019

Ng, W.-T., Rima, P., Einzmann, K., Immitzer, M., Atzberger, C., & Eckert, S. (2017). Assessing the Potential of Sentinel-2 and Pléiades Data for the Detection of Prosopis and Vachellia spp. in Kenya. *Remote Sensing*, *9*(1), 74. https://doi.org/10.3390/rs9010074

Otkin, J. A., Anderson, M. C., Hain, C., Mladenova, I. E., Basara, J. B., & Svoboda, M. (2013). Examining rapid onset drought development using the thermal infrared–based Evaporative Stress Index. *Journal of Hydrometeorology*, *14*(4), *1057–1074*, https://doi.org/10.1175/JHM-D-12-0144.1

Orwa, C., Mutua, A., Kindt, R., Jamnadass, R., Simons, A. (2009). *Prosopis glandulosa*. Agroforestree Database: a tree reference and selection guide version 4.0. World Agroforestry Centre, Kenya. https://apps.worldagroforestry.org/treedb2/speciesprofile.php?Spid=1353

OZ Leads Major Renovations of the Historic "Oasis at Death Valley." (2018). OZ Architecture. Retrieved February 10, 2025. https://ozarch.com/insights/5631

Parker, S., Moore, J., & Warren, L. (2018). *Ecological Values of the Amargosa River in California*. https://www.scienceforconservation.org/products/ecological-values-of-the-amargosa/

Pavelko, M. T., & Damar, N. A. (2023). *Groundwater discharge by evapotranspiration from the Amargosa Wild and Scenic River and contributing areas, Inyo and San Bernardino Counties, California* (No. 2023-5106). US Geological Survey. https://doi.org/10.3133/sir20235106

Weather - Death Valley National Park (U.S. National Park Service). (2024, May 15). https://www.nps.gov/deva/planyourvisit/weather.htm

8. Appendices

Appendix A: *Vegetation Health*

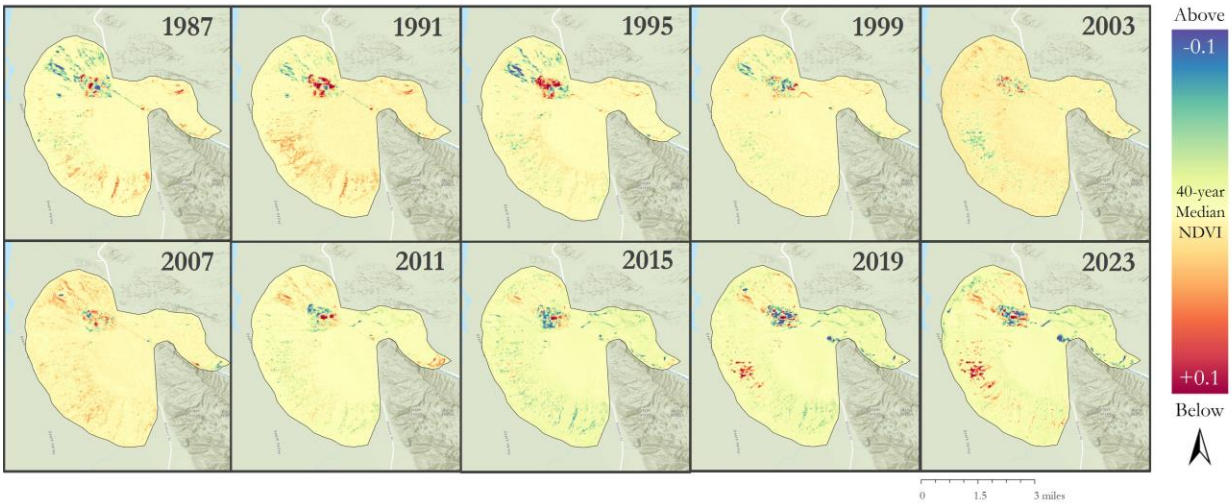

Figure A1. Historical NDVI anomalies from the overall, 40-year NDVI median from Landsat 4, 5, 8, and 9.

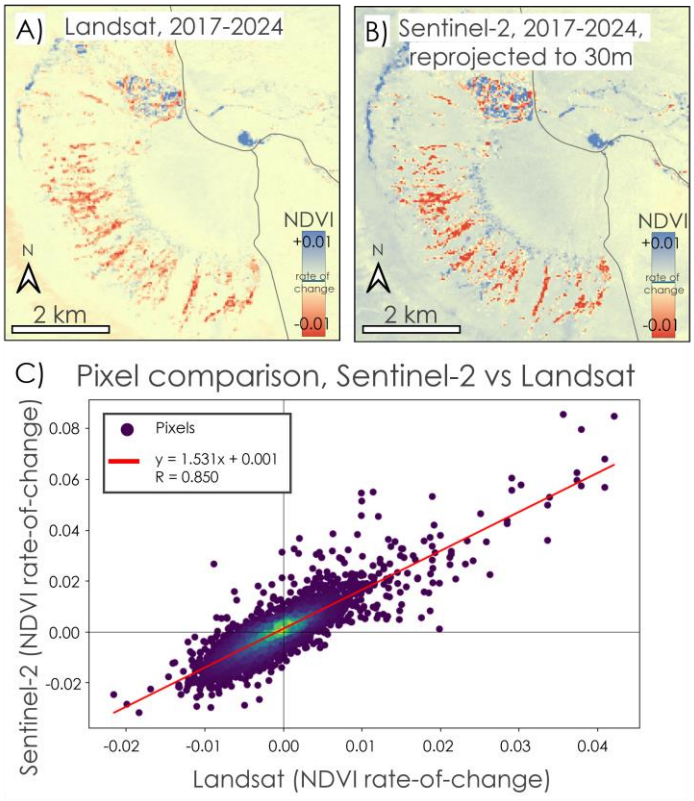

Figure A2. Comparing NDVI rate-of-change from (**A**) Landsat vs (**B**) Sentinel-2 over the same time frame, 2017 to 2024, with Sentinel-2 pixels resampled to 30m by averaging. The graph (**C**) shows the pixel-by-pixel comparison, excluding non-vegetation pixels that do not have an NDVI value greater than 0.1 for any of the years. The points are colored by density of points from low density purple to high density green and yellow. This highlights that the greatest density of points center around 0 NDVI-rate-of-change.

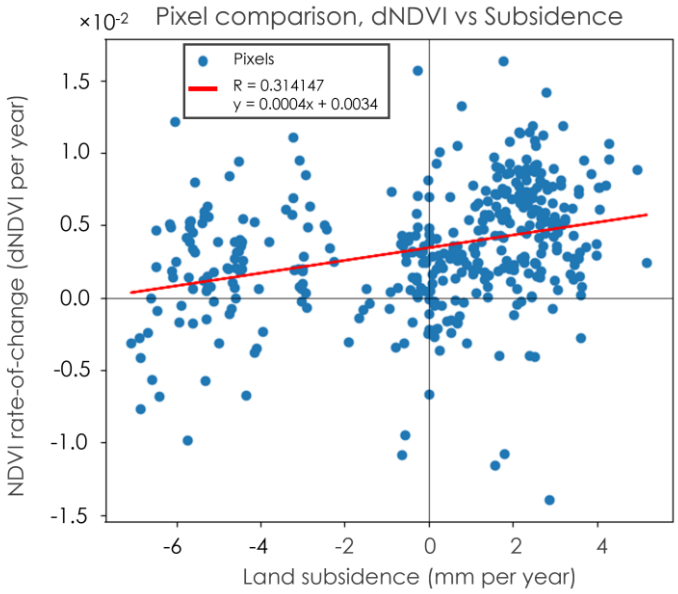

Figure A3. Pixel-by-pixel comparison between Sentinel-2 NDVI rate-of-change from 2017–2024 vs average land subsidence across the entire Amargosa Basin including Death Valley National Park. Each ~1-km pixel is plotted as a blue dot, while the line-of-best-fit is in red. Note the y-axis is scaled by 10^{-2}. The coefficient of correlation, or R value, signifying the strength of correlation between the NDVI rate-of-change and land subsidence is 0.314147 out of 1, indicating a weak-moderate correlation.

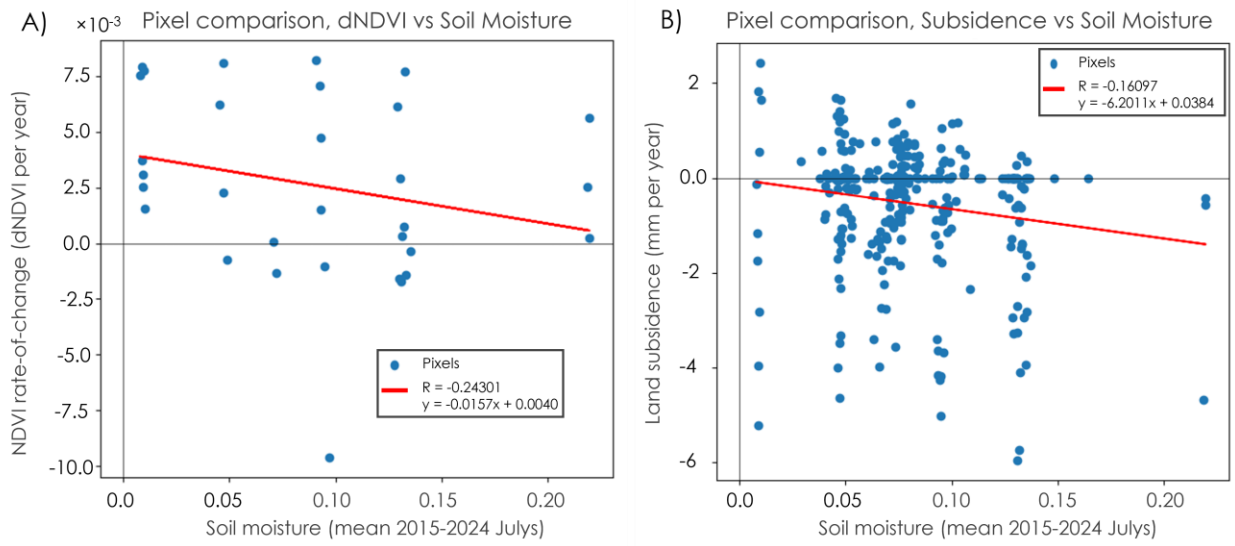

Figure A4. Pixel-by-pixel comparison between average soil moisture and A) Sentinel-2 NDVI rate-of-change from 2017–2024 or B) land subsidence in mm per year from 2015–2019 across the entire Amargosa Basin including Death Valley National Park. Each ~9-km pixel is plotted as a blue dot, while the line-of-best-fit is in red. Note the y-axis in A) is scaled by 10^{-3}. The coefficient of correlation, or R value, signifies the strength of correlation. Neither comparison shows correlation.

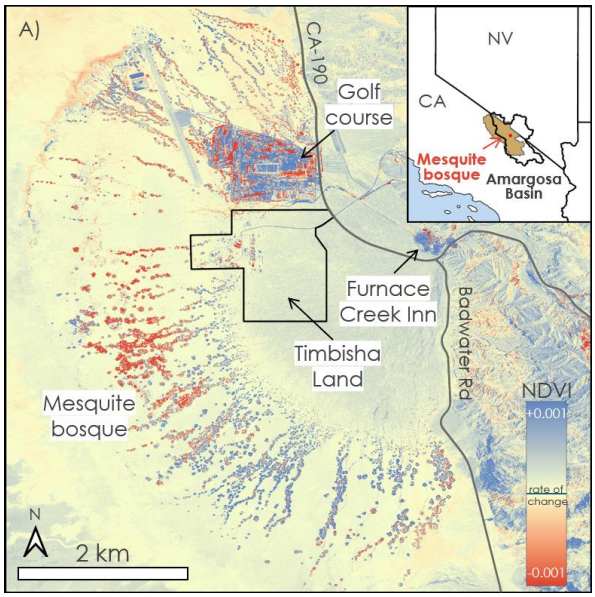

Figure A5. Rate-of-change map for NAIP-derived NDVI from 2012–2022.

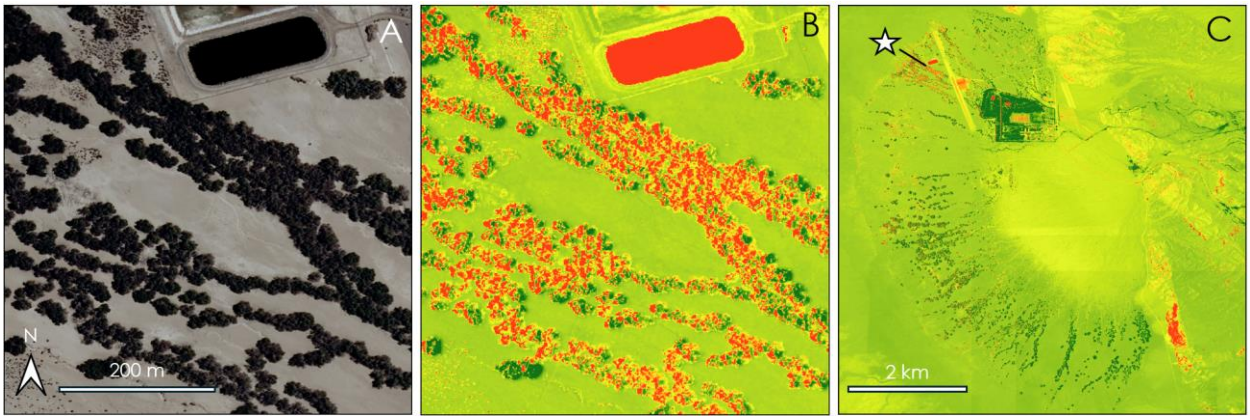

Figure A6. True color imagery (A) and NDVI (B) from NAIP in 2010, with a map showing the location of this area within the Furnace Creek (C). NDVI values were unexpectedly negative over what appeared to be healthy mesquite, possibly due to shadows as this phenomenon was most observed on the western sides of mesquite trees. This year was excluded from rate-of-change calculations for NAIP-derived NDVI.

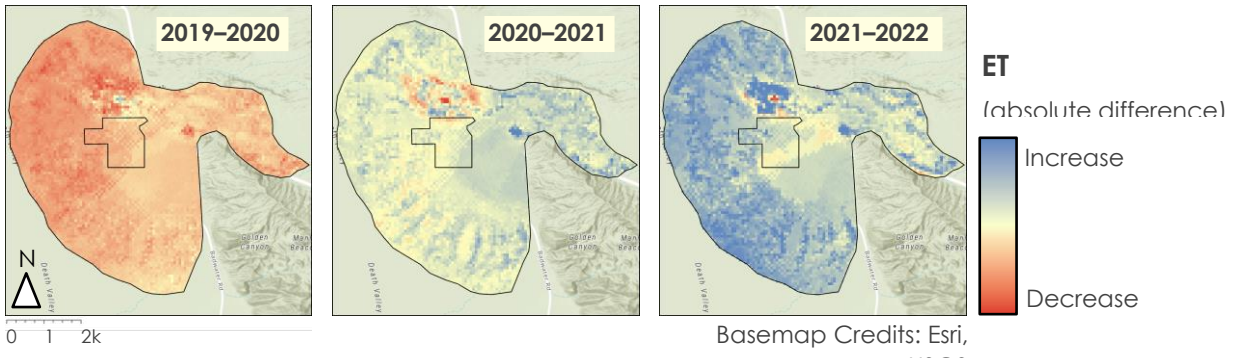

Figure A7. Absolute difference in ET values between years to identify areas that experienced either a net increase or decrease in productivity. Blue indicates a net increase in plant productivity whereas red indicates a net decrease in productivity. The midtone color approximates no change in ET value.

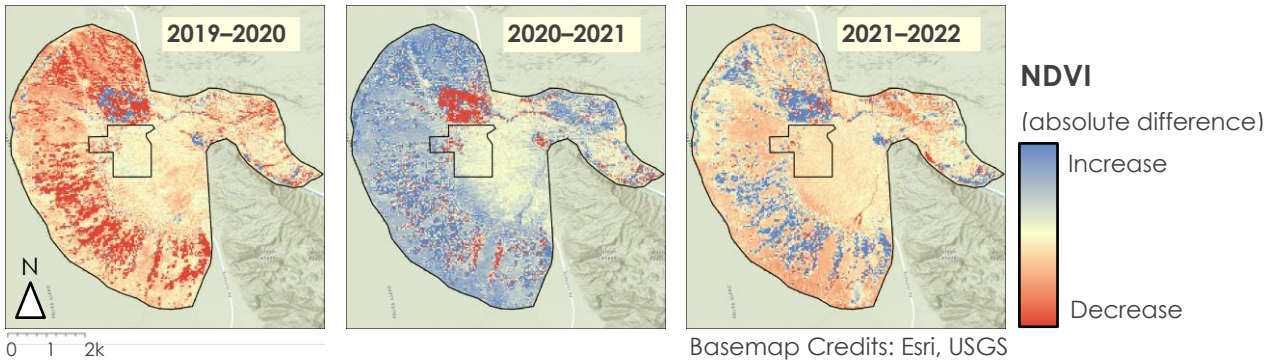

Figure A8. Absolute difference in NDVI values between the observed years for ET years to identify areas that experienced either a net increase or decrease in vegetation health. Blue indicates a net increase in NDVI whereas red indicates a net decrease in NDVI. The midtone color approximates no change in NDVI value.

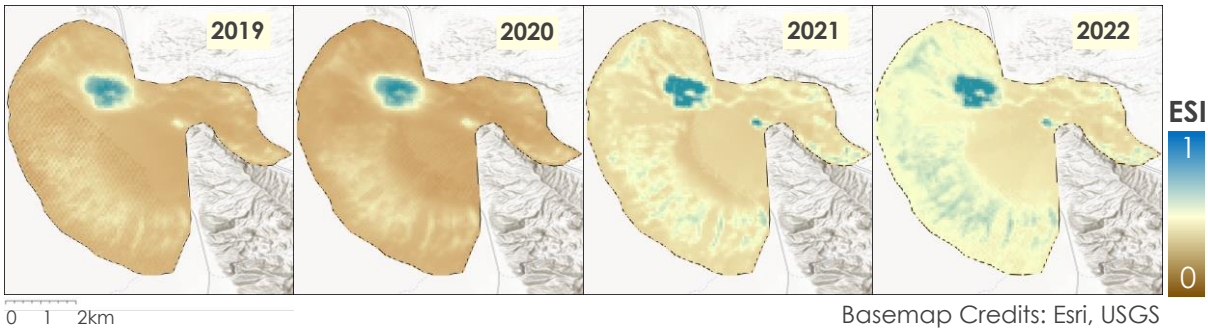

Figure A9. Furnace Creek mesquite bosque ESI over 2019–2022 at 70-m resolution from ISS ECOSTRESS. A value closer to 1 indicates vegetation is less stressed and more productive while values closer to 0 are more stressed and less productive.

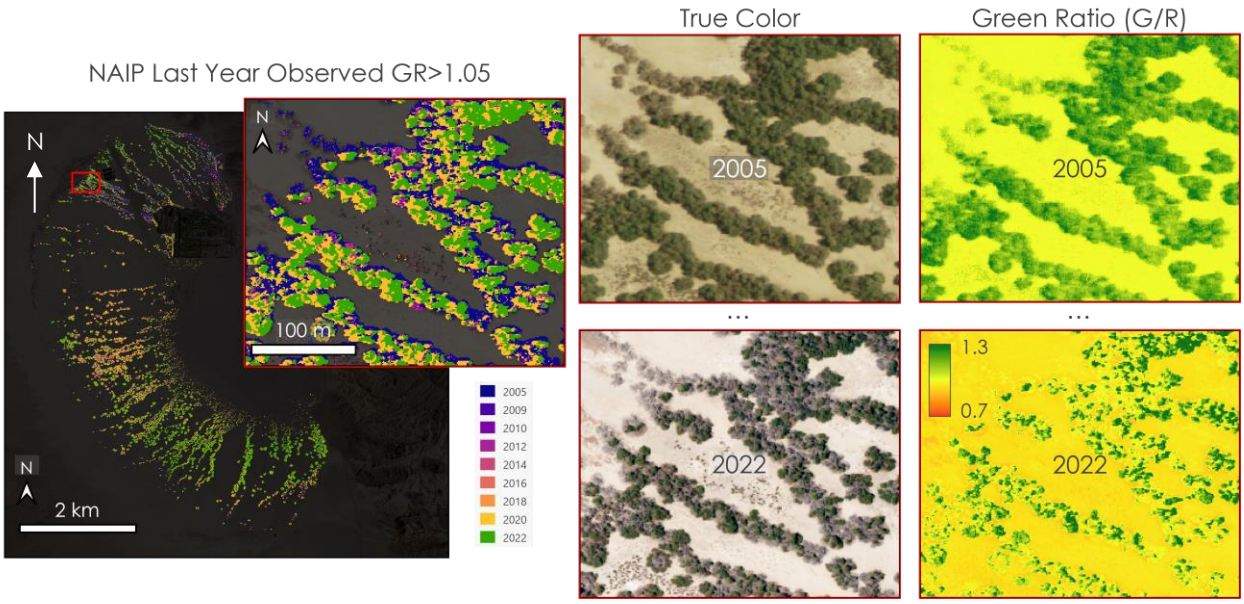

Figure A10. NAIP Green Ratio (GR). The left map shows Furnace Creek with an inset red box. This map shows the last year that the green ratio was greater than 1.05 from 2005 through 2022. The green ratio is demonstrated in the right 4 maps showing true color and green ratio images for the same area in 2005 and 2022, where there is a clear decline in green foliage, reflected in the green ratio counterpart images.

Appendix B: Hydrology

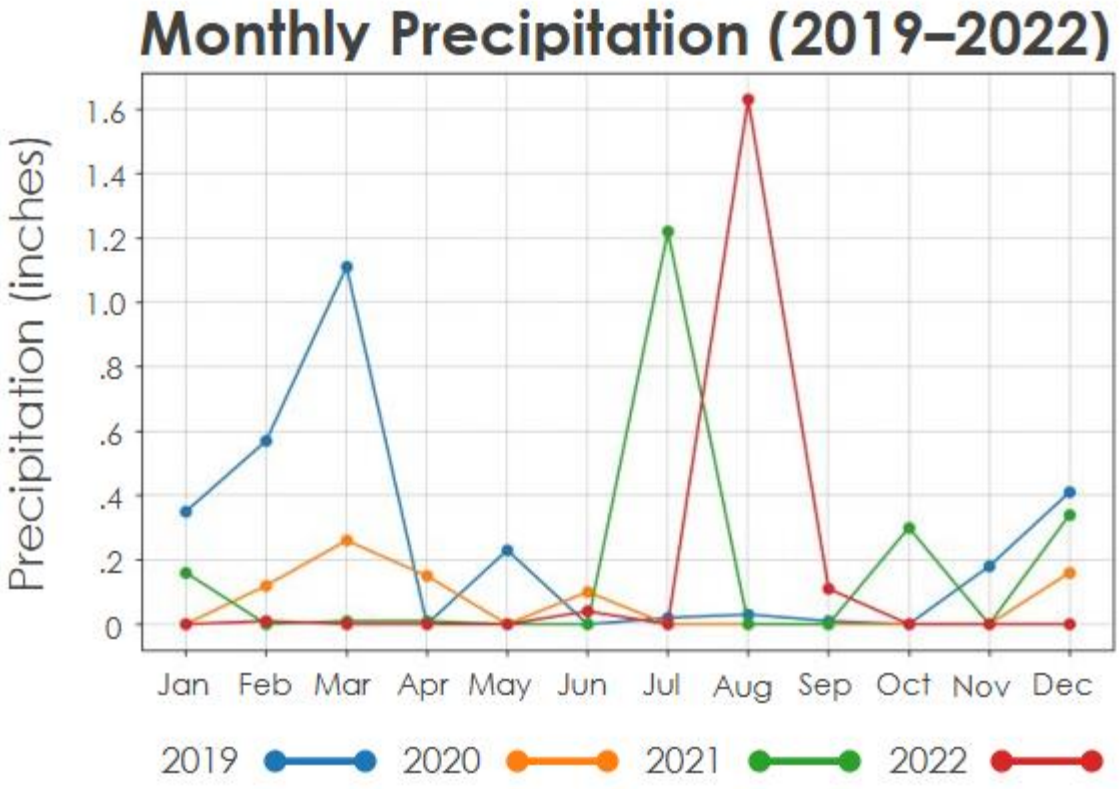

Figure B1. Furnace Creek precipitation monthly averages from 2019 to 2022.